Simple computation of the eigencomponents of a subdivision matrix in the Fourier domain

Loïc Barthe[1], Cédric Gérot[2], Malcolm A. Sabin[3], and Leif Kobbelt[4]

[1] Computer Graphics Group, IRIT/UPS, 118 route de Narbonne, 31062 Toulouse Cedex4, France. lbarthe@irit.fr
[2] Laboratoire des Images et des Signaux, Domaine Universitaire, 38402 Saint Martin D'Heres, France. Cedric.Gerot@lis.inpg.fr
[3] Numerical Geometry ltd., 26 Abbey Lane, Lode, Cambridge, UK. malcolm@geometry.demon.co.uk
[4] Computer Graphics Group, RWTH Aachen, Ahornstrasse 55, 52074 Aachen, Germany. kobbelt@cs.rwth-aachen.de

Summary. After demonstrating the necessity and the advantage of decomposing the subdivision matrix in the frequency domain when analysing a subdivision scheme, we present a general framework based on the method introduced in [1] which computes the Discrete Fourier Transform of a subdivision matrix. The effectivity of the technique is illustrated by perfoming the analysis of Kobbelt's $\sqrt{3}$ scheme in a very simple manner.

1 Introduction

Nowadays, subdivision surfaces have become a standard technique for both animation and freeform shape modeling [21]. After *one* step of subdivision, a coarse mesh is refined to a finer one and several iterations generate a sequence of incrementally refined meshes which converge to a smooth surface. The main advantage of subdivision surfaces on other freeform representations such as splines [9] is that they are defined by control meshes with arbitrary connectivity while generating smooth surfaces with arbitrary manifold topology. One of the most important stages in subdivision scheme analysis is the evaluation of the scheme's smoothness properties. This is done in *two* steps:

First, one has to study the continuity properties of the scheme in a regular lattice (composed of valence 6 vertices for triangles meshes and valence 4 vertices for quad meshes). Often the scheme is derived from the uniform knot-insertion operator of some Box-spline surface [2] which leads us to a trivial analysis: By construction the refined meshes converge to piecewise polynomial surfaces with a known degree of smoothness between the patches [3, 5, 11]. On the other hand, the scheme can be non-polynomial [8, 22, 10], i.e. it is not

derived from any known surface representation and the continuity of the limit surface is analysed using sufficient conditions based on z-Transforms [6, 10, 7].

As the second step in the analysis, one has to analyse the scheme's smoothness in the vicinity of extraordinary vertices (EVs). Up to now, the z-Transform fails to provide an efficient tool at EVs, and even though we can prove C^1 continuity for schemes derived from Box-splines by showing that the characteristic map is regular and injective [15, 12, 20], the complete analysis is performed using necessary conditions based on the eigenstructure of the subdivision matrix [5, 1, 16]. In fact, the convergence behavior of a subdivision scheme at an EV is completely determined by the eigencomponents of its subdivision matrix. The analysis of a subdivision scheme [5, 11, 19, 14, 10] in the vicinity of such irregularities of the control mesh hence requires a simple technique for identifying and computing the various eigencomponents. The standard method exploits the scheme's rotational symmetries through the use of the Fourier transform. This partitions the subdivision matrix, which size varies linearly with the valence of the EV, into a block diagonal matrix. Although the number of blocks depends on the valence, the blocks are of fixed size, and so it becomes possible to determine the eigencomponents for all valences with a single algebraic computation.

In this paper, we first illustrate by a practical example the importance of the frequency analysis and we emphasize the necessity of identifying the eigenvalues with respect to their rotational frequency. We then present the general form of Ball and Story's method [1] which performs a fast computation of the different frequency blocks. This approach is illustrated on Kobbelt's $\sqrt{3}$ scheme [10] and we show how very simple computations performed on a single subdivision iteration rather than on the square of the subdivision matrix allow us to deal with the scheme's rotation property and to find the specific subdivision rules for the EVs.

Another method computing the eigencomponents of a subdivision matrix is based on z-Transforms and it exploits the circulant structure of the subdivision matrix' blocks. This technique also leads to very simple computations and all details can be found in [12, 18]. Both methods are equivalent in terms of complexity, however our method computes the eigencomponents in the Fourier domain while the use of z-Transforms provides the eigencomponents in the spacial domain. Depending on the application, one or the other method can be prefered.

2 Frequency of the different eigenvalues

The operator which maps a central EV of valence v and its r-ring neighborhood $\mathbf{P}$ to the same topological configuration $\mathbf{p}$ after *one* step of subdivision is called the subdivision matrix S. The vectors of old vertices $\mathbf{P}$ and new vertices $\mathbf{p}$ are linked by the relation $\mathbf{p} = S\mathbf{P}$. The matrix S is square and each of its rows contains the coefficients of an affine combination of the old vertices $\mathbf{P}$

which computes *one* new vertex of $\mathbf{p}$. The convergence behavior of the subdivision scheme at the central EV is completely defined by the eigencomponents (eigenvalues and eigenvectors) of the matrix S. The matrix S is then decomposed into $S = M\,\Lambda\,M^{-1}$ where Λ is a diagonal matrix of eigenvalues $\{\lambda_j\}$ and M is a square matrix whose columns are the (*right*) eigenvectors $\mathbf{m_j}$. This can be well understood if we interpret the eigencomponents as a local Taylor expansion. Indeed, this interpretation allows us to associate the different geometric configurations (position, tangent plane, curvature) with the eigencomponents by which they are defined. The smoothness analysis then relies on necessary conditions for the eigencomponents of the different geometric configurations.

As we will see in Section 2.1, given the mere eigendecomposition of a subdivision matrix, we cannot directly deduce which eigenvalue corresponds to which geometric configuration so that we do not know how to apply the conditions for the scheme's smoothness analysis. In Section 2.2 we show how the decomposition of the subdivision matrix in the Fourier domain resolves this problem.

2.1 Geometric configurations and their eigencomponents

The Taylor expansion of a function $f : \mathbb{R}^2 \to \mathbb{R}$ can be written as follows:

$$\begin{aligned} f(x,y) = f + f_x\,x + f_y\,y + (f_{xx} + f_{yy})\left(\frac{x^2}{4} + \frac{y^2}{4}\right) \\ + (f_{xx} - f_{yy})\left(\frac{x^2}{4} - \frac{y^2}{4}\right) + f_{xy}\,xy + \ldots \quad , \end{aligned} \tag{1}$$

where each function expression on the right hand side is evaluated at $(0,0)$. The point f is a position, the *two* first order partial derivatives f_x and f_y are the coefficients of x and y defining the tangent plane and the *three* second order partial derivatives f_{xx}, f_{yy} and f_{xy} are the coefficients of three quadratic configurations defining the curvature: An elliptic configuration x^2+y^2 denoted as *cup* and *two* rotationally symmetric hyperbolic configurations $x^2 - y^2$ and $x\,y$ denoted as *saddle*.

On the other hand, the vector of new vertices $\mathbf{p}$ is expressed as a local Taylor expansion when it is computed as $\mathbf{p} = S\,\mathbf{P} = M\,\Lambda\,M^{-1}\,\mathbf{P} = M\,\Lambda\,\mathbf{l}$ with $\mathbf{l} = M^{-1}\mathbf{P}$ [13]. We then have:

$$\mathbf{p} = \mathbf{m_0}\,\lambda_0\,l_0 + \mathbf{m_1}\,\lambda_1\,l_1 + \mathbf{m_2}\,\lambda_2\,l_2 + \mathbf{m_3}\,\lambda_3\,l_3 + \mathbf{m_4}\,\lambda_4\,l_4 + \mathbf{m_5}\,\lambda_5\,l_5 + \ldots \quad , \tag{2}$$

where the $l_j \in \mathbb{R}^3$ are the approximations of the Taylor coefficients, i.e., the successive partial derivatives (l_0 is a position, l_1 and l_2 approximate the first order derivatives, etc), the $\mathbf{m_j}$s correspond to the polynomials in Eq. (1),

whose function values scale with a certain factor λ_j. Eq. (1) and (2) both behave like local Taylor expansions applied in different contexts. They have identical geometric interpretation and in Eq. (2), the components $\mathbf{m_j}$, λ_j and l_j with index $j = 0$ are responsible for the central EV's position, components with indices $j = 1, 2$ are responsible for the tangent plane and those with indices $j = 3, 4, 5$ are responsible for the curvature: $j = 3$ for the cup and $j = 4, 5$ for the *two* saddles.

Note that the components with indices $j = 1, 2$ defining the tangent plane configuration are images under rotation, yielding the property $|\lambda_1| = |\lambda_2|$. This is also the case for the *two* saddle configurations which yields $|\lambda_4| = |\lambda_5|$.

The study of the subdivision scheme's smoothness at the EV is based on necessary conditions affecting the different eigencomponents $\{\lambda_j\}$ and $\{\mathbf{m}_j\}$. For instance, the condition $1 = |\lambda_0| > |\lambda_j|$ for all $j > 0$ is necessary for convergence of the scheme, the additional conditions $1 > |\lambda_1|$, $1 > |\lambda_2|$ and $\min(|\lambda_1|, |\lambda_2|) > |\lambda_j|$ for $j > 2$ are necessary for C^1 continuity and if the scheme is C^1. However, in practice, useful schemes are rotationally symmetric and therefore we restrict our analysis to this special case. This gives us the additional properties : $|\lambda_1| = |\lambda_2|$ and $|\lambda_4| = |\lambda_5|$. Properties like bounded curvature ($|\lambda_2|^2 \geq |\lambda_3|$, $|\lambda_2|^2 \geq |\lambda_4| = |\lambda_5|$ and $\min(|\lambda_3|, |\lambda_4|) > |\lambda_j|$ for $j > 5$) are necessary for C^2 continuity. If $|\lambda_2|^2 = |\lambda_3| = |\lambda_4| = |\lambda_5|$, the scheme has a *non-zero* bounded curvature (without flat spot at the EV) and if $|\lambda_2|^2 > |\lambda_j|$, $j = 3, 4, 5$, the scheme has *zero* curvature generating a flat spot at the EV.

A critical point in the analysis after eigendecomposition of the subdivision matrix is then to identify which index (or configuration) corresponds to which eigencomponents. Since we know which eigenvalue corresponds to which eigenvector, the task is reduced to the identification of the different eigenvalues. This is illustrated by the following example:

Let us consider a variant of Loop's subdivision scheme [11] having its n-uplet of eigenvalues $(\lambda_0, ..., \lambda_7)$ at a valence 7 EV sorted by geometric configuration (following our Taylor notation (2)) and having their value in the set:

$$\{1, \frac{1}{2}, \frac{1}{2}, \frac{1}{4}, \frac{1}{4}, \frac{1}{4}, \lambda_j < \frac{1}{4}\} \tag{3}$$

We emphasize that the set of eigenvalues is not sorted sorted from the greatest to the smallest as it is usually done, but by geometric configuration. The question is: How can we know which one of the eigenvalues in (3) is λ_0, λ_1,... ? Indeed, following (2), each order satisfies different properties. For instance, the eigenvalues can have the following values:

$$(\lambda_0, \lambda_1, \lambda_2, \lambda_3, \lambda_4, \lambda_5, \lambda_6, \lambda_7) = (1, \frac{1}{2}, \frac{1}{2}, \frac{1}{4}, \frac{1}{4}, \frac{1}{4}, <\frac{1}{4}, <\frac{1}{4}), \tag{4}$$

and hence one can deduce that the scheme is certainly C^1 and that it has bounded curvature. If indeed the analysis of the caracteristic map proves C^1

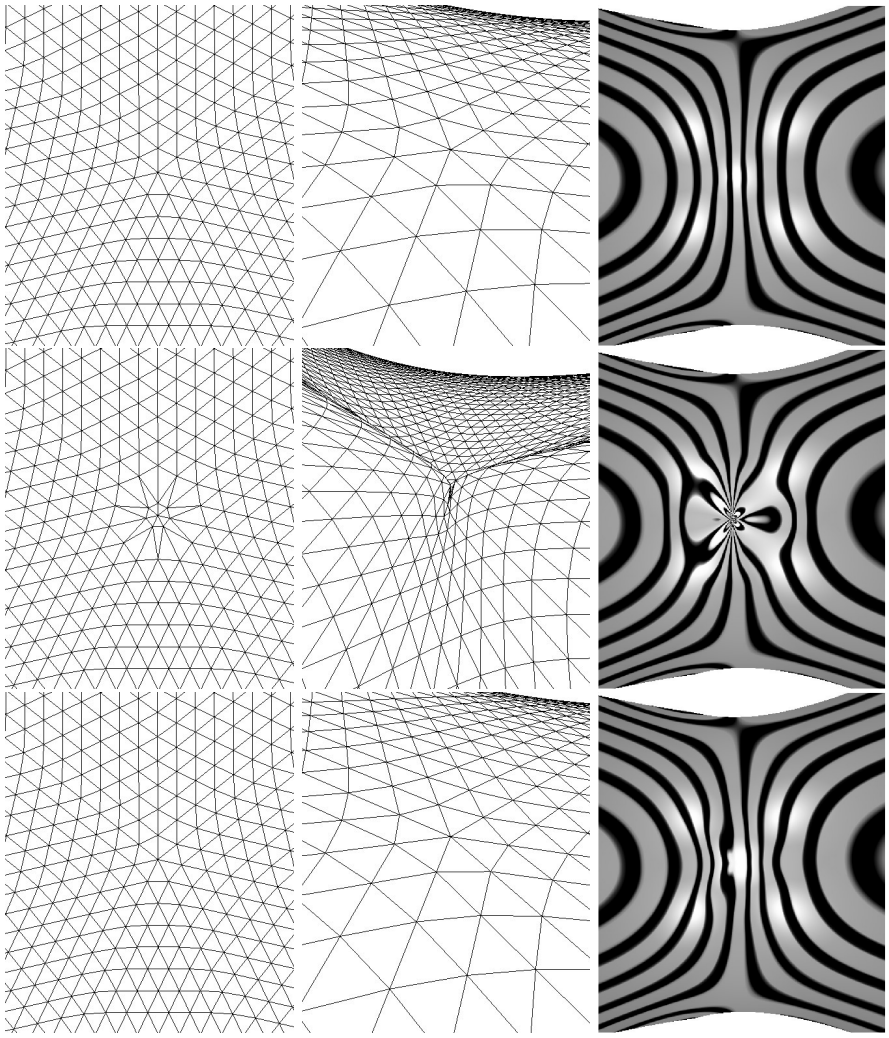

Fig. 1. Different versions of Loop's scheme at a valence 7 EV. The first column shows the subdivision of a semi-regular planar mesh with the EV in its center. The second column shows a subdivided saddle mesh with the EV in its center and the third column illustrates the curvature behavior using reflexion lines on the same saddle mesh. In the first row, the scheme has the eigenspectrum (4) and it is C^1 continuous with non-*zero* bounded curvature (no flat spot). In the second row, it has the eigenspectrum (5). We clearly see the shrinking factor of $\lambda_1 = \lambda_2 = \frac{1}{4}$ at the EV in the planar configuration and the C^1 discontinuity in the saddle mesh. In the third row it has the eigenspectrum (6) and the scheme is C^1 continuous with bounded curvature (flat spot in the saddle configuration). The misbehavior of the curvature is illustrated by the reflexion lines in the saddle mesh.

continuity, the scheme is C^1 at the EV and it has bounded curvature without flat spot (first row in Fig. 1). However if the eigenvalues are actually:

$$(\lambda_0, \lambda_1, \lambda_2, \lambda_3, \lambda_4, \lambda_5, \lambda_6, \lambda_7) = (1, \frac{1}{4}, \frac{1}{4}, \frac{1}{4}, \frac{1}{2}, \frac{1}{2}, < \frac{1}{4}, < \frac{1}{4}), \tag{5}$$

the necessary condition for C^1 continuity is not satisfied ($|\lambda_2| < |\lambda_4|$) so that the scheme is not C^1 and it is not even necessary to analyse the characteristic map (second row in Fig. 1). Finally, the situation where :

$$(\lambda_0, \lambda_1, \lambda_2, \lambda_3, \lambda_4, \lambda_5, \lambda_6, \lambda_7) = (1, \frac{1}{2}, \frac{1}{2}, \frac{1}{4}, \lambda_4 < \frac{1}{4}, \lambda_5 < \frac{1}{4}, \frac{1}{4}, \frac{1}{4}), \tag{6}$$

is more problematic because if the analysis of the characteristic map proves that the scheme is C^1, one could conclude from the eigenspectrum (3) that it has also bounded curvature without flat spot at the EV ($|\lambda_1|^2 = |\lambda_2|^2 = |\lambda_3| = |\lambda_4| = |\lambda_5|$) while it is not the case. In the saddle configuration, the curvature is bounded with a flat spot, and some curvature misbehavior can be introduced in the limit surface by the eigenvectors corresponding to the eigenvalues λ_6 and λ_7 (third row in Fig. 1).

The decomposition of the subdivision matrix in the Fourier domain will allow us to determine if we are in the situation (4), (5), (6) or in a situation where the eigenvalues are sorted in a still different manner.

2.2 Identification of the eigenvalues in the Fourier domain

The identification of the eigenvalues is based on the decomposition of the subdivision matrix S in the Fourier domain. The block circulant subdivision matrix S with n blocks $S_{i,j}$ is transformed into a block diagonal matrix $\tilde{S}$ having v blocks $\tilde{S}_\omega$ which correspond to the *rotational frequencies* $\omega = \{0, .., v-1\}$ ordered in frequency in $\tilde{S}_\omega$ (as illustrated in Equation (7)). We define the *rotational frequency* just below. The eigenvalues of the frequency blocks $\tilde{S}_\omega$ are amplitudes of the eigenvalues of the matrix S [1, 17], hence if we know which frequency represents each configuration (position, tangent plane, cup and saddle), we can identify the eigenvalues from the frequency block in which they are computed.

$$S = \left[\begin{array}{c|ccc} & & & \\ \hline & S_{0,0} & \cdots & S_{0,n} \\ \hline & \vdots & \ddots & \vdots \\ & \vdots & \ddots & \vdots \\ \hline & S_{n,0} & \cdots & S_{n,n} \end{array}\right] \longrightarrow \tilde{S} = \begin{bmatrix} [\,\tilde{S}_0\,] & & & 0 \\ & [\,\tilde{S}_1\,] & & \\ & & \ddots & \\ 0 & & & [\,\tilde{S}_{v-1}\,] \end{bmatrix} \tag{7}$$

In the Taylor expansion (1), the constant term refers to a position, the terms for x and y define the tangent plane and terms in x^2+y^2, x^2-y^2 and xy define the different curvature configurations (cup and *two* saddles). The expression of these configurations in a cylindrical coordinate system (Eq. (8)) as a periodic function $g(\theta) = \rho\cos(\omega\,\theta+\varphi)$ (where ρ is the amplitude, ω is the frequency and φ is the phase) provides directly the rotational frequency ω associated to each configuration. For instance, $x^2-y^2 = r^2\cos(2\theta)$ and hence this saddle configuration has a frequency component $\omega = 2$. Note that due to rotational symmetry, $\tilde{S}_\omega = \tilde{S}_{v-\omega}$ so that it is enough to consider the frequencies $\omega = \{0,..,\frac{v}{2}\}$.

$$(x,y,z) \rightarrow (r,\theta,z) \qquad \text{with} \qquad \begin{cases} x = r\cos(\theta) \\ y = r\sin(\theta) \\ z = z \end{cases} \tag{8}$$

This tells us that the position configuration has the frequency $\omega = 0$ and hence the eigenvalue $|\lambda_0|$ is the dominant eigenvalue of the frequency block $\tilde{S}_0$, the tangent plane configuration has the frequency $\omega = 1$ and $|\lambda_1| = |\lambda_2|$ equals the dominant eigenvalue $\tilde{\mu}_1$ of the frequency block $\tilde{S}_1$, the cup configuration has the frequency $\omega = 0$ and $|\lambda_3|$ equals the subdominant eigenvalue $\tilde{\mu}_0$ of the frequency block $\tilde{S}_0$ and finally the saddle configurations have the frequency $\omega = 2$ and $|\lambda_4| = |\lambda_5|$ equals the dominant eigenvalue $\tilde{\mu}_2$ of the frequency block $\tilde{S}_2$. This relation between the different eigencomponents and their rotational frequencies is presented in [5].

When a scheme is convergent, its eigenvalue λ_0 equals 1 (Sect. 2.1) and since $|\lambda_0|$ is the dominant eigenvalue of the frequency block $\tilde{S}_0$, it can be written as:

$$\tilde{S}_0 = \begin{bmatrix} 1 & \cdots \\ 0 & \left[\,\tilde{S}_0'\,\right] \end{bmatrix}. \tag{9}$$

In this paper, we only consider convergent subdivision schemes, and so $\lambda_0 = 1$ and the cup eigenvalue $|\lambda_3|$ is the dominant eigenvalue $\tilde{\mu}_0$ of the block $\tilde{S}_0'$.

3 Computation of the frequency blocks

In this section, we present a general framework, used in [1] on Catmull-Clark's scheme [3], which computes the eigencomponents in the frequency domain. We present the procedure on a triangular lattice with a 2-ring neighborhood around the central EV and a standard dyadic refinement (see Fig. 2(a)). The adaptation to a single 1-ring neighborhood or to quad meshes [1] is straightforward. We notice that this method may not be suitable to analyse non-rotationally symmetric schemes, however, as pointed out in [4], these schemes are mainly interesting for theoretical studies and all the schemes used in practical applications are rotationally symmetric.

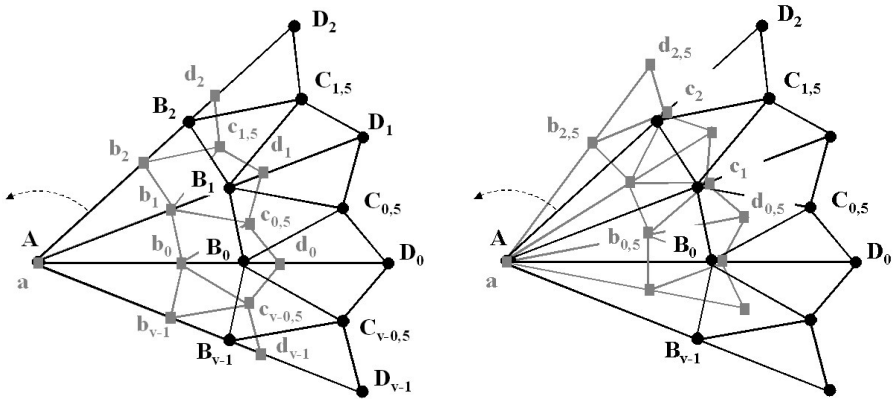

Fig. 2. Subdivision with (a) a dyadic refinement and (b) a $\sqrt{3}$ refinement, of a 2-ring configuration around a central EV A of valence v. Capital letters denote the set of old vertices $\mathbf{P}$ and small letters the set of new vertices $\mathbf{p}$.

The set of old vertices $\mathbf{P}$ is defined as follows:

$$\mathbf{P} = \{A, B_0, .., B_{v-1}, C_{\frac{1}{2}}, .., C_{v-\frac{1}{2}}, D_0, .., D_{v-1}\},$$

where the different letters $X = \{B, C, D\}$ denote the different sets of rotationally symmetric vertices around the central EV A and the indices give the rotational position of each vertex: Vertex X_j is at an angle of $\frac{j\,2\,\pi}{v}$ (where v is the valence of the EV) from the axis of origin. The set of new vertices $\mathbf{p}$:

$$\mathbf{p} = \{a, b_0, .., b_{v-1}, c_{\frac{1}{2}}, .., c_{v-\frac{1}{2}}, d_0, .., d_{v-1}\},$$

represents the same topological configuration, but after *one* step of subdivision and around the central EV a. The new vertices of $\mathbf{p}$ are computed using affine combinations g_k^j of the old vertices of $\mathbf{P}$:

$$a = g^0(\mathbf{P}), \quad b_k = g_k^1(\mathbf{P}), \quad c_{k+\frac{1}{2}} = g_k^2(\mathbf{P}), \quad d_k = g_k^3(\mathbf{P}), \quad k = 0, .., v-1,$$

where the affine combinations g_k^j are the rows of the subdivision matrix S.

Using the Discrete Fourier Transform (DFT):

$$\tilde{x}_\omega = \frac{1}{v} \sum_{l=0}^{v-1} x_l \exp(-2\pi i \omega l / n), \quad x = \{a, b, c, d\}, \tag{10}$$

we express the rotational frequencies $\{\tilde{a}_\omega, \tilde{b}_\omega, \tilde{c}_\omega, \tilde{d}_\omega\}$ of each set of rotationally symmetric new vertices of $\mathbf{p}$ in terms of the rotational frequencies $\tilde{\mathbf{P}}_\omega = \{\tilde{A}_\omega, \tilde{B}_\omega, \tilde{C}_\omega, \tilde{D}_\omega\}$ of the old vertices of $\mathbf{P}$:

$$\tilde{a}_\omega = \tilde{g}^0_\omega(\tilde{\mathbf{P}}_\omega), \quad \tilde{b}_\omega = \tilde{g}^1_\omega(\tilde{\mathbf{P}}_\omega), \quad \tilde{c}_\omega = \tilde{g}^2_\omega(\tilde{\mathbf{P}}_\omega), \quad \tilde{d}_\omega = \tilde{g}^3_\omega(\tilde{\mathbf{P}}_\omega),$$

where the affine combinations $\tilde{g}^j_\omega$ are the rows of the frequency blocks $\tilde{S}_\omega$ of the discrete Fourier transform $\tilde{S}$ of the subdivision matrix S. In vertices A and a, the only frequency is the *zero* frequency, hence the terms in $\exp(-2\pi i\omega l/v)$ vanish in the expression of $\tilde{a}_\omega$ and we have: $A = \tilde{A}_0 = \tilde{A}$, $a = \tilde{a}_0 = \tilde{a}$ and $\forall\,\omega > 0$, $\tilde{A}_\omega = \tilde{a}_\omega = 0$. Furthermore, in order to express the frequency block $\tilde{S}_0$ as in Equation (9), we have to center the analysis at the central EV so that:

$$\begin{bmatrix} \tilde{a}_0 \\ \tilde{b}_0 - \tilde{a}_0 \\ \tilde{c}_0 - \tilde{a}_0 \\ \tilde{d}_0 - \tilde{a}_0 \end{bmatrix} = \begin{bmatrix} & \tilde{S}_0 & \\ & & \end{bmatrix} \begin{bmatrix} \tilde{A}_0 \\ \tilde{B}_0 - \tilde{A}_0 \\ \tilde{C}_0 - \tilde{A}_0 \\ \tilde{D}_0 - \tilde{A}_0 \end{bmatrix} \text{ with } \begin{bmatrix} \tilde{S}_0 \end{bmatrix} = \begin{bmatrix} 1 & \cdots \\ 0 & \begin{bmatrix} \tilde{S}'_0 \end{bmatrix} \end{bmatrix},$$

hence

$$\begin{bmatrix} \tilde{b}_0 - \tilde{a}_0 \\ \tilde{c}_0 - \tilde{a}_0 \\ \tilde{d}_0 - \tilde{a}_0 \end{bmatrix} = \begin{bmatrix} & \tilde{S}'_0 & \\ & & \end{bmatrix} \begin{bmatrix} \tilde{B}_0 - \tilde{A}_0 \\ \tilde{C}_0 - \tilde{A}_0 \\ \tilde{D}_0 - \tilde{A}_0 \end{bmatrix},$$

and because for $\omega > 0$: $\tilde{A}_\omega = \tilde{a}_\omega = 0$, $\forall\,\omega > 0$ we have:

$$\begin{bmatrix} \tilde{b}_\omega \\ \tilde{c}_\omega \\ \tilde{d}_\omega \end{bmatrix} = \begin{bmatrix} & \tilde{S}_\omega & \\ & & \end{bmatrix} \begin{bmatrix} \tilde{B}_\omega \\ \tilde{C}_\omega \\ \tilde{D}_\omega \end{bmatrix}.$$

The size of the frequency blocks is equal to the number of sets of rotationally symmetric vertices in the neigborhood of the central EV. Hence, these blocks are of fixed size (here they are 3×3 matrices) and they can be expressed as a function of the valence v of the central EV. The original problem of computing the eigencomponents of large $(3v+1) \times (3v+1)$ matrices (*in the spatial domain*) for each value of the valence v is reduced to a single eigendecomposition of small 3×3 matrices (*in the Fourier domain*), providing the different eigencomponents expressed in terms of the valence v. Depending on their complexity, the frequency blocks can be either decomposed by hand computations or using the symbolic toolbox of any mathematical software.

We note that the right eigenvectors $\tilde{\mathbf{m}}_\mathbf{0}$, $\tilde{\mathbf{m}}_\mathbf{1}$ and $\tilde{\mathbf{m}}_\mathbf{2}$ associated respectively to the eigenvalues $\tilde{\mu}_0$, $\tilde{\mu}_1$ and $\tilde{\mu}_2$, can be interpreted as amplitudes of the eigenvectors $\mathbf{m_0}, .., \mathbf{m_5}$ of the spatial domain, e.g. the tangent plane eigenvector $\tilde{\mathbf{m}}_\mathbf{1} = [r_B, r_C, r_D]$ gives the radii r_X of vertices B_k, $C_{k+\frac{1}{2}}$ and D_k from the central EV A.

4 Example by Kobbelt's $\sqrt{3}$ scheme

We illustrate by the practical example of Kobbelt's $\sqrt{3}$ subdivision scheme [10] the application of the general procedure presented in Sect. 3. This scheme rotates the lattice after *one* step of subdivision due to the insertion of new vertices in the middle of the old faces (as we can see in Fig. 2(b)). If the eigendecomposition is performed on the subdivision matrix S, we obtain complex eigencomponents generated by the scheme's rotation property. To overcome this difficulty, in [10] the scheme is rather analysed after *two* steps of subdivision so that the lattice is aligned with the *two* steps older one but rotated by *one* sector. The lattice is then rotated back using a permutation matrix R, and the matrix studied finally is $\hat{S} = R\,S^2$.

We first compute the frequency blocks on the 2-ring configuration shown in Fig. 2(b). The computation is performed on a single subdivision step without any back-rotation. We then reproduce the results presented in [10] using the eigencomponents in the Fourier domain. We will see that the computations are so simple that they can be done quickly and easily by hand.

Kobbelt's $\sqrt{3}$ scheme is composed of *two* refinement rules (*stencils*): One which displaces an old vertex (Eq. (11)) and one which computes a new vertex in the center of a triangle (Eq. (12)). They are defined by the following formulae:

$$a = (1 - \alpha_v)A + \frac{\alpha_v}{v}\sum_{j=0}^{v-1} B_j \tag{11}$$

$$b_{k+\frac{1}{2}} = \frac{1}{3}(A + B_k + B_{k+1}), \tag{12}$$

where α_v is a parameter which can be used in order to improve the surface smoothness at the EV for different valences v. The new vertices c_k are computed using the regular relaxation rule (valence 6 vertex) and the new vertices $d_{k+\frac{1}{2}}$ using the insertion rule as follows:

$$\begin{aligned} c_k &= \frac{2}{3}B_k + \frac{1}{18}(A + B_{k-1} + B_{k+1} + C_{k-\frac{1}{2}} + C_{k+\frac{1}{2}} + D_k) \\ d_{k+\frac{1}{2}} &= \frac{1}{3}(B_k + B_{k+1} + C_{k+\frac{1}{2}}). \end{aligned}$$

The DFT (Eq. (10)) is then used to derive the rotational frequencies of the different sets of rotationally symmetric vertices:

$$\begin{aligned}
\tilde{a}_0 &= 1.\sum_{j=0}^{0} a\, e^0 = (1-\alpha_v)A + \frac{\alpha_v}{v}\sum_{j=0}^{v} B_j \quad \text{using the DFT and Eq. (11)}\\
&= (1-\alpha_v)\tilde{A}_0 + \alpha_v \tilde{B}_0 \quad \text{because the only frequency in } a \text{ is } \omega = 0\\
\tilde{b}_\omega &= \frac{1}{v}\sum_{j=0}^{v-1} b_j\, e^{-2\pi i\omega j/v} \quad \text{DFT}\\
&= \frac{1}{v}\sum_{j=0}^{v-1}\left[\frac{1}{3}(A + B_{j-\frac{1}{2}} + B_{j+\frac{1}{2}})\right] e^{-2\pi i\omega j/v} \quad \text{using Eq. (12)}\\
&= \frac{1}{3}A + \frac{1}{3v}\sum_{l=-\frac{1}{2}}^{v-\frac{3}{2}} B_l\, e^{-2\pi i\omega\left(l+\frac{1}{2}\right)/v} + \frac{1}{3v}\sum_{l=\frac{1}{2}}^{v-\frac{1}{2}} B_l\, e^{-2\pi i\omega\left(l-\frac{1}{2}\right)/v}\\
&= \frac{1}{3}A + \frac{1}{3v}e^{-2\pi i\omega/2v}\sum_{l=-\frac{1}{2}}^{v-\frac{3}{2}} B_l\, e^{-2\pi i\omega l/v} + \frac{1}{3v}e^{2\pi i\omega/2v}\sum_{l=\frac{1}{2}}^{v-\frac{1}{2}} B_l\, e^{-2\pi i\omega l/v}\\
&= \frac{1}{3}\tilde{A}_0 + \frac{1}{3}\left(e^{-\pi i\omega/v} + e^{\pi i\omega/v}\right)\tilde{B}_\omega\\
&= \frac{1}{3}\tilde{A}_0 + \frac{2}{3}k_\omega\tilde{B}_\omega \quad \text{with } k_\omega = \cos\left(\frac{\pi\omega}{v}\right) \text{ and because } e^{-i\theta} + e^{i\theta} = 2\cos\theta
\end{aligned}$$

hence

$$\begin{cases} \tilde{b}_0 - \tilde{a}_0 = \left(\frac{2}{3} - \alpha_v\right)\left(\tilde{B}_0 - \tilde{A}_0\right) & \text{if } \omega = 0\\ \tilde{b}_\omega = \frac{2}{3}k_\omega\tilde{B}_\omega & \text{otherwise.}\end{cases}$$

Using similar computations, we obtain:

$$\begin{cases} \tilde{c}_0 - \tilde{a}_0 = \left(\frac{7}{9} - \alpha_v\right)\left(\tilde{B}_0 - \tilde{A}_0\right) + \frac{1}{9}\left(\tilde{C}_0 - \tilde{A}_0\right) + \frac{1}{18}\left(\tilde{D}_0 - \tilde{A}_0\right) & \text{if } \omega = 0\\ \tilde{c}_\omega = \left(\frac{2}{3} + \frac{1}{9}k_{2\omega}\right)\tilde{B}_\omega + \frac{1}{9}k_\omega\tilde{C}_\omega + \frac{1}{18}\tilde{D}_\omega & \text{otherwise}\end{cases}$$

$$\begin{cases} \tilde{d}_0 - \tilde{a}_0 = \left(\frac{2}{3} - \alpha_v\right)\left(\tilde{B}_0 - \tilde{A}_0\right) + \frac{1}{3}\left(\tilde{C}_0 - \tilde{A}_0\right) & \text{if } \omega = 0\\ \tilde{d}_\omega = \frac{2}{3}k_\omega\tilde{B}_\omega + \frac{1}{3}\tilde{C}_\omega & \text{otherwise.}\end{cases}$$

From these expressions, we directly deduce the frequency blocks:

$$\tilde{S}'_0 = \begin{bmatrix} \frac{2}{3} - \alpha_v & 0 & 0\\ \frac{7}{9} - \alpha_v & \frac{1}{9} & \frac{1}{18}\\ \frac{2}{3} - \alpha_v & \frac{1}{3} & 0 \end{bmatrix} \text{ and if } \omega > 0 \quad \tilde{S}_\omega = \begin{bmatrix} \frac{2}{3}k_\omega & 0 & 0\\ \frac{2}{3} + \frac{1}{9}k_{2\omega} & \frac{1}{9}k_\omega & \frac{1}{18}\\ \frac{2}{3}k_\omega & \frac{1}{3} & 0 \end{bmatrix}.$$

Since the only non-zero coefficient of the first rows of the matrices $\tilde{S}'_0$ and $\tilde{S}_\omega$ is the one in the left-hand corner, we directly obtain the dominant eigenvalues $\tilde{\mu}_0$, $\tilde{\mu}_1$ and $\tilde{\mu}_2$ as:

$$\tilde{\mu}_0 = \frac{2}{3} - \alpha_v, \qquad \tilde{\mu}_1 = \frac{2}{3}k_1, \qquad \tilde{\mu}_2 = \frac{2}{3}k_2. \tag{13}$$

As we see, the free parameter α_v only appears in the cup eigenvalue, hence the scheme's behavior is improved at the EV by bounding the curvature in the cup configuration using the condition: $\tilde{\mu}_0 = \tilde{\mu}_1^2$. The value of parameter α_v in Eq. (11) is then derived as follows:

$$\tilde{\mu}_0 = \tilde{\mu}_1^2 \quad \Longleftrightarrow \quad \frac{2}{3} - \alpha_v = \left(\frac{2}{3}k_1\right)^2 \quad \Longleftrightarrow \quad \alpha_v = \frac{2}{9}\left(2 - \cos\left(\frac{2\pi}{v}\right)\right).$$

The eigenvalues $\tilde{\mu}_i$ $(i = 1, 2, 3)$ could have been computed in an even simpler manner by only considering a 1-ring neigborhood around the central EV. However, the choice of a 2-ring neighborhood is based on our wish of giving an example allowing a more complete analysis based on a larger neighborhood. It also allows us to check that more eigenvalues are adequately sorted (see the necessary conditions on the eigenvalues in Sect. 2.1).

5 Conclusion

In this paper, we have emphasized the importance of the analysis of the subdivision matrix in the Fourier domain: The analysis of large matrices in the spatial domain is reduced to the analysis of small matrices in the Fourier domain so that it becomes easier to compute the different eigencomponents. Moreover, we can determine which geometric configuration is defined by which eigencomponents. We have presented a general framework computing the subdivision matrix in the frequency domain and it has been illustrated on the practical example of Kobbelt's $\sqrt{3}$ scheme. We have shown how this computation technique allows us to analyse the scheme in a very simple manner.

There are limitations for this computation technique when the rotational position of a set of rotationally symmetric vertices with respect to the axis of origin is unknown. More investigations have to be carried out to solve this problem while keeping the computations as simple as possible. As we have demonstrated however, this approach performs on 2-ring neigborhood configurations and hence it is very well suited to analyse most of the standard subdivision schemes or any new rotationally symmetric scheme.

References

[1] Ball, A.A., Storry, D.J.T.: Conditions for tangent plane continuity over recursiveley generated B-spline surfaces. ACM Transactions on Graphics, **7** (2), 83–102 (1988)

[2] de Boor, C., Hollig, D., Riemenschneider, S.: Box Splines. Springer-Verlag, New York (1994).

[3] Catmull, E., Clark, J.: Recursively generated B-spline surfaces on arbitrary topological meshes. Computer Aided Design, 10 (6), 350–355 (1978)

[4] Dodgson N.A., Ivrissimtzis, I.P., Sabin, M.A.: Characteristics of dual triangular $\sqrt{3}$ subdivision. Curves and Surface Fitting: Saint-Malo 2002, Nashboro Press, Brentwood, 119–128 (2003)

[5] Doo, D., Sabin, M.A.: Analysis of the behaviour of recursive subdivision surfaces near extraordinary points. Computer Aided Design, **10** (6), 356–360 (1978)

[6] Dyn, N.: Subdivision schemes in Computer-Aided Geometric Design. Advances in Numerical Analysis, **II**, Wavelets, Subdivision Algorithms and Radial Basis Functions, W. Light (ed.), Clarendon Press, Oxford, 36–104 (1992)

[7] Dyn, N.: Analysis of convergence and smoothness by the formalism of Laurent polynomials. Tutorials on Multiresolution in Geometric Modelling, A. Iske, E. Quak and M. Floater (ed.), Springer, 51–68 (2002)

[8] Dyn, N., Levin, D., Gregory, J.: A butterfly subdivision scheme for surface interpolation with tension control. ACM Transaction on Graphics, **9** (2) 160–169 (1990)

[9] Farin, G.: Curves and Surfaces for CAGD. 5^{th} Edition, Academic Press (2002)

[10] Kobbelt, L.: $\sqrt{3}$-Subdivision. Proceedings of SIGGRAPH 2000, Computer Graphics Proceedings, Annual Conference Series, ACM, 103–112 (2000)

[11] Loop, C.: Smooth subdivision surfaces based on triangles. Master's thesis, University of Utah (1987)

[12] Peters, J., Reif, U.: Analysis of algorithms generalizing B-spline subdivision. SIAM Journal of Num. Anal., 35 (2), 728–748 (1998)

[13] Prautzsch, H.: Analysis of Ck-Subdivision surfaces at extraordinary points. Technical Report 98/4, Fakultät für Informatik, University of Karlsruhe, Germany (1998)

[14] Prautzsch, H., Umlauf, G.: A G^2-subdivision algorithm. Geometric Modelling, Dagstuhl 1996, Computing supplement 13, Springer-Verglas, 217–224 (1998)

[15] Reif, U.: A unified approach to subdivision algorithms near extraordinary vertices. Computer Aided Design, 12, 153–174 (1995)

[16] Sabin, M.A.: Eigenanalysis and artifacts of subdivision curves and surfaces. Tutorials on Multiresolution in Geometric Modelling, A. Iske, E. Quak and M. Floater (ed.), Springer, 69–97 (2002)

[17] Stam, J.: Exact evaluation of Catmull-Clark subdivision surfaces at arbitrary parameter values. Proceedings of SIGGRAPH 1998, ACM, 395–404 (1998)

[18] Warren, J., Weimer, H.: Subdivision methods for geometric design: A constructive approach. San Francisco: Morgan Kaufman, (2002)

[19] Zorin, D.: Stationary subdivision and multiresolution surface representations. PhD thesis, Caltech, Pasadena, California (1997)
[20] Zorin, D.: A method for analysis of C^1-continuity of subdivision surfaces. SIAM Journal of Num. Anal., 35 (5), 1677–1708 (2000)
[21] Zorin, D., Schröder, P: Subdivision for modeling and animation. SIGGRAPH 2000 Course Notes. (2000)
[22] Zorin, D., Schröder, P., Sweldens, W.: Interpolating subdivision for meshes with arbitrary topology. Proceedings of SIGGRAPH 1997, ACM, 189–192 (1996)